(7) (a) C. S. Cundy, M. Green, and F. G. A. Stone, *J. Chem. Soc. A*, 1647 (1970); (b) F. G. A. Stone, *Pure Appl. Chem.*, **30**, 551 (1972).

(8) A. Greco, M. Green, S. K. Shakshooki, and F. G. A. Stone, *Chem. Commun.*, 1374 (1970).

(9) E. P. Kündig, M. Moskovits, and G. A. Ozin, *J. Mol. Struct.*, **14**, 137 (1972).

(10) M. Moskovits and G. A. Ozin, *J. Appl. Spectrosc.*, **26**, 487 (1972).

(11) (a) T. Shimanouchi, *J. Chem. Phys.*, **26**, 594 (1957); (b) G. Hertzberg, "Molecular Spectra and Molecular Structure", Vol. II, 2nd ed, D. van Nostrand, Princeton, N.J., 1960.

(12) (a) G. Fogarasi, *Acta Chim. Acad. Sci. Hung.*, **66**, 87 (1970); (b) K. Ramaswamy and V. Devarajan, *J. Mol. Struct.*, **8**, 325 (1971); (c) J. K. Brown and K. J. Morgan, *Adv. Fluorine Chem.*, **4**, 253 (1965); (d) A. Monfils and J. Duchesne, *J. Chem. Phys.*, **18**, 1415 (1950); (e) P. Torkington and H. W. Thompson, *Trans. Faraday Soc.*, **41**, 237 (1945); (f) J. R. Nielsen, H. H. Claassen, and D. C. Smith, *J. Chem. Phys.*, **18**, 817 (1950).

(13) (a) C. R. Brundle, M. B. Robin, N. A. Kruebler, and H. Basch, *J. Am. Chem. Soc.*, **94**, 1451 (1972); (b) C. B. Duke, K. L. Yip, G. P. Ceasar, A. W. Potts, and D. G. Streets, *J. Chem. Phys.*, **66**, 256 (1977); (c) W. M. Flicker, Ph.D. Thesis, California Institute of Technology, 1976.

(14) E. P. Kündig, M. Moskovits, and G. A. Ozin, *Angew. Chem., Int. Ed. Engl.*, **14**, 292 (1975).

(15) L. Hanlan, H. Huber, E. P. Kündig, B. McGarvey, and G. A. Ozin, *J. Am. Chem. Soc.*, **97**, 7054 (1975).

(16) T. A. Clarke, I. D. Gay, and R. Mason, "The Physical Basis for Heterogeneous Catalysis", E. Drauglis and R. I. Jaffee, Ed., Plenum Press, New York and London, 1975.

(17) (a) H. H. Hoehn, L. Pratt, K. F. Watterson, and G. Wilkinson, *J. Chem. Soc.*, 2738 (1961); (b) T. A. Manuel, S. L. Stafford, and F. G. A. Stone, *J. Am. Chem. Soc.*, **83**, 249 (1961).

(18) J. A. Evans and J. C. Tatlow, *J. Chem. Soc.*, 3779 (1954).

(19) K. Klabunde, private communication.

(20) N. Rösch and R. Hoffmann, *Inorg. Chem.*, **13**, 2656 (1974).

(21) (a) R. G. Denning, F. R. Hartley, and L. M. Venanzi, *J. Chem. Soc. A*, 1322 (1967); (b) D. J. Trecker, J. P. Henry, and J. E. McKeon, *J. Am. Chem. Soc.*, **87**, 3261 (1965); (c) T. N. Murrel and S. Carter, *J. Chem. Soc.*, 6185 (1964).

(22) (a) W. J. Power, manuscript in preparation; (b) H. Huber, D. McIntosh and G. A. Ozin, *Inorg. Chem.*, in press.

(23) H. Huber, G. A. Ozin, and W. J. Power, *Inorg. Chem.*, **16**, 979 (1977).

(24) We note that the perfluoronickelacyclopropane ring system has recently been stabilized in the complex tetrafluoroethylene-1,1,1-tris(diphenylphosphinomethyl)ethanenickel. A crystal structure analysis of the complex established that the phosphine ligand is *tridentate* through three phosphorus atoms; the coordinated $C_2F_4$ group is highly distorted, each $CF_2$ being bent away from the planar conformation by an average of 42° (J. Browning and B. R. Penfold, *J. Chem. Soc., Chem. Commun.*, 198 (1973). This compound can be considered to be analogous to the complex tetrafluoroethylene-*t*,*t*,*t*-cyclododeca-1,5,9-trienenickel[8] which is also stable to ring expansion. These observations support Stone's conviction[8] that the ring expansion requires coordination of the second unsaturated molecule.

(25) Maples, M. Green, and F. G. A. Stone, *J. Chem. Soc., Dalton Trans.*, 388 (1973).

(26) G. A. Ozin, *Catal. Rev.*, in press; *Acc. Chem. Res.*, **10**, 21 (1977), and references cited therein.

(27) General valence bond and configuration interaction calculations for both ($\pi$-$C_2H_4$)Ni and ($\pi$-$C_2H_4$)$Ni_2$ have recently been performed and provide a detailed insight into the bonding and electronic properties of these types of binary transition-metal olefin complexes; G. A. Ozin, W. J. Power, W. A. Goddard III, and T. Upton, *J. Am. Chem. Soc.*, in press.

---

Contribution from the Lash Miller Chemistry Laboratory and Erindale College, University of Toronto, Toronto, Ontario, Canada, and Department of Chemistry, University of Washington, Seattle, Washington 98195

# Bimetal Atom Chemistry. 1. Synthesis, Electronic Absorption Spectrum, and Extended Hückel/Self-Consistent Field-X$\alpha$-Scattered Wave Molecular Orbital Analyses of the CrMo Molecule; Relevance to Alloy and Bimetallic Cluster Catalysis

WERNER KLOTZBÜCHER, GEOFFREY A. OZIN,*[†] JOE G. NORMAN, JR.,* and HAROLD J. KOLARI

*Received March 18, 1977*

AIC70213M

The simultaneous cocondensation of Cr atoms and Mo atoms with low-temperature argon matrices at 10 K provides a controlled synthetic pathway to the heteronuclear diatomic molecule CrMo. Mixed-metal concentration, UV–visible experiments enable the electronic absorptions of CrMo to be identified in the presence of the parent diatomics, $Cr_2$ and $Mo_2$. Extended Hückel and SCF-X$\alpha$-SW molecular orbital techniques are employed to probe the electronic and bonding properties of CrMo. Both methods indicate that the heteronuclear molecule has properties essentially intermediate between those of the corresponding homonuclear molecules (a similar suggestion has recently been made for the $\sigma$–$\sigma$* transition energies of discrete, heteronuclear metal–metal bonded complexes). The relevance of this type of "few-atom data" to the more complex problem of alloy and bimetallic cluster catalysis is also briefly considered.

## Introduction

Incentives for experimental and theoretical research in the field of small, well-defined metal clusters often originate with problems in the fields of chemisorption and heterogeneous catalysis.[1-6] One question of paramount importance concerns the number of metal atoms required by a cluster for it to display characteristic bulk properties. Here one is inquiring into the dependence of the electronic, molecular, and chemical properties of a collection of metal atoms as a function of cluster size and geometry. The development of reliable techniques for handling this type of problem is crucial as the outcome impinges directly on our way of thinking about electronic factors in catalysis,[2,3] structure sensitivity of catalytic reactions,[2,4] localized bonding models of the chemisorbed state,[2,5] and alloy and bimetallic catalysis,[2,6] to name but a few.

Some of the essential experimental groundwork in the field of few-atom clusters is now being laid mainly as a result of recent breakthroughs in metal atom matrix techniques.[7] The isolation and measurement of the electronic spectra of the molecules $Sc_2$,[8] $Ti_2$,[9] $Cr_2$,[10a] $Cr_3$,[10b] $Mn_2$,[11] $Fe_2$,[11a] $Fe_{3,4}$,[11b] $Co_{2,3}$,[12] $Ni_2$,[11a,13] $Ni_3$,[13b] $Cu_2$,[14a] $Nb_2$,[15] $Mo_2$,[15] $Mo_3$,[10b] $Rh_2$,[16] $Pd_2$,[17] $Ag_2$,[14b] $Ag_{2,3,4,5,6,7}$[14c] attests to the success of the method. With the emergence of such complete sets of experimental data, the theoretician can begin to answer fundamental questions relating to metal–metal bond orders and the extent of d vs. s vs. p orbital contributions to the bonding in transition-metal diatomic molecules.

Historically, the deliberate cryochemical synthesis and spectroscopic characterization of small, naked metal clusters began only a few years ago.[10a] During some experiments with Cr atoms it was discovered that quantitative UV-visible monitoring of the surface diffusion processes of metal atoms in low-temperature matrices provided a means of identifying the various clusters that form in the embryonic stages of metal aggregation. Using this method, $Cr_2$[10a] and subsequently $Mo_2$[15] were generated and their electronic absorptions identified. Independent confirmation of these assignments came recently from observations of gaseous $Cr_2$ and $Mo_2$ generated by flash photolysis of $Cr(CO)_6$ and $Mo(CO)_6$.[18] Although the mechanism of formation of the gaseous diatomics is not obvious, the close agreement between the flash photolysis[18] and matrix data[10a,15] is particularly gratifying.

---

* To whom correspondence should be addressed: G. A. Ozin, University of Toronto; J. G. Norman, Jr., University of Washington.

[†] Sherman-Fairchild Distinguished Scholar (1977), California Institute of Technology, Pasadena, Calif. 91125.

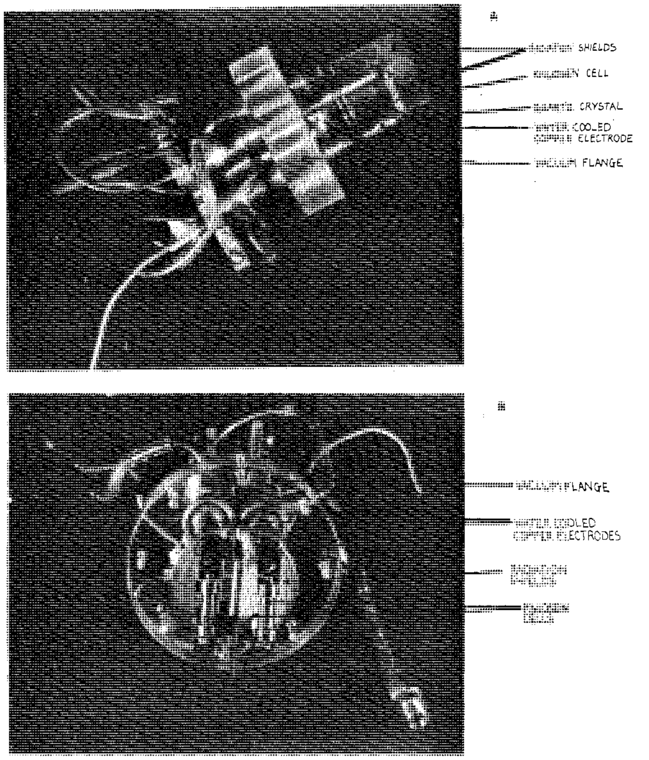

**Figure 1.** Photograph of the four-electrode vacuum flange and dual quartz crystal microbalance assembly (A) side view and (B) front view, used for mixed Cr atom, Mo atom matrix depositions with simultaneous monitoring of the individual metal flows. (The resolution of the microbalance is approximately $10^{-8}$ g.[20])

Just as accurate electronic spectral information for transition-metal, homonuclear diatomic molecules provides a useful reference point for theoretical studies of the chemisorptive and catalytic properties of larger metal aggregates, it is our contention that the corresponding data for heteronuclear diatomics will prove to be equally valuable for theoretically modeling "alloy" clusters as a function of size, geometry, and composition. Therefore in this particular study we have extended our earlier $Cr_2$, $Mo_2$ experiments[10a,15] to demonstrate for the first time that the *simultaneous* cocondensation of two different metal atomic vapors with low-temperature matrices can provide a controlled synthetic route to heteronuclear diatomic clusters. In these first experiments we have been able to generate CrMo and measure its UV–visible absorption spectrum in Ar matrices. Extended Hückel and SCF-X$\alpha$-SW molecular orbital techniques are employed to probe the electronic and bonding properties of this interesting diatomic. Finally the relevance of this type of data to the more complex problem of alloy and bimetallic cluster catalysis is examined. The following is a detailed account of these investigations.

## Results and Discussion

To perform metal atom matrix cocondensation experiments[19] with two different metal atomic vapors we employed a specially designed, four-electrode vacuum furnace containing two independent quartz crystal microbalances.[20] A photograph of the vacuum flange–electrode–crystal oscillator assembly is shown in Figure 1. The individual Cr atom and Mo atom deposition rates were calibrated by establishing the flow conditions required to produce (i) isolated Cr (or Mo) atoms and (ii) Cr (or Mo) atoms in the presence of $Cr_2$ (or $Mo_2$) molecules (see ref 10a and 15 for details of the Cr/$Cr_2$ and Mo/$Mo_2$ matrix experiments). It is worth noting here that the UV–visible spectral assignments for $Cr_2$ and $Mo_2$ based on our earlier quantitative metal concentration experiments have recently been confirmed by gas-phase flash photolysis studies of $Cr(CO)_6$ and $Mo(CO)_6$.[18] We recall here that a particularly striking feature of the $Cr_2$ (Figure 2A) and $Mo_2$ (Figure 2B) matrix spectra is an intense, sharp, low-energy absorption at 460 and 516 nm, respectively (band I). Weaker absorptions are observed at 340/263 nm for $Cr_2$ and at 308/232 nm for $Mo_2$[10a,15] (bands II and III). Careful examination of the 232-nm band of $Mo_2$ under high-concentration, high-ordinate expansion conditions reveals a weak shoulder at roughly 226 nm that had not previously been noticed.[15] Similarly, a weak shoulder at 268 nm is observed on the 263-nm band of $Cr_2$ (see Figure 3 and later discussion). Other very weak bands indicated by an asterisk in Figure 3 are unassigned as it is not possible with the available data to define them as belonging to binuclears or higher clusters.

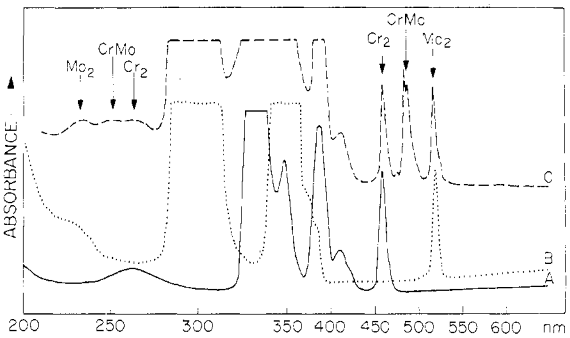

**Figure 2.** The UV–visible absorption spectrum of the products of the matrix deposition (A) Cr/Ar $\simeq$ 1/1000, (B) Mo/Ar $\simeq$ 1/1000, and (C) Cr/Mo/Ar $\simeq$ 1/1/1000 at 10 K showing the bands of $Cr_2$, $Mo_2$, and CrMo molecules in the presence of Cr and Mo atoms.

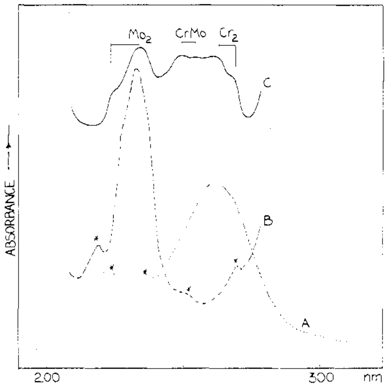

**Figure 3.** The same as Figure 2C but showing an expansion of the high-energy (band III) region of $Cr_2$/CrMo/$Mo_2$. (The asterisks indicate unassigned bands (see text and Table I).)

The results of a typical mixed Cr/Mo atom matrix cocondensation experiment with Cr/Mo/Ar $\simeq$ 1/1/1000 are displayed in Figure 2C. A new and remarkably clear spectral feature can now be observed at 485/488 nm [Careful examination of this region of the spectrum revealed what appears to be vibronic structure on the CrMo absorption. Six components were observed (Figure 4) with an average vibrational spacing of 147 $cm^{-1}$.] which is essentially "midway" between the corresponding electronic absorptions of $Cr_2$/$Mo_2$ at 460/516 nm, respectively. Weaker spectral features at 322 and 248 nm appear to have the same growth characteristics as the new species giving rise to the 485/488 nm absorption. Moreover, they lie at frequencies intermediate between the 340/308 nm and 263/232 nm absorptions of $Cr_2$/$Mo_2$, respectively.

A series of Cr/Mo/Ar metal concentration experiments was performed in the range $1/1/10^4$ to $1/1/10^2$ at 10 K and indicated that, besides the known absorptions of Cr/Mo and $Cr_2$/$Mo_2$, only those of the new species at 485/488, 322, and 248 nm remain to be accounted for. Having previously es-

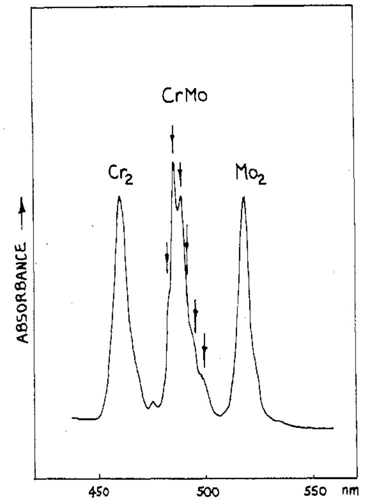

**Figure 4.** The same as Figure 2C but showing an expansion of the low-energy (band I) region of $Cr_2/CrMo/Mo_2$.

**Table I.** Electronic Absorption Spectra of Matrix Isolated and Gaseous $Cr_2$, CrMo, and $Mo_2$ Molecules[a]

| Cr/Mo atom matrix cocondensations[b] | $Cr(CO)_6/Mo(CO)_6$ flash photolysis[c] | Assignment of obsd bands |
|---|---|---|
| 516 | 520 | $Mo_2$ |
| 487[d] | 480 | CrMo |
| 460 | 460 | $Cr_2$ |
| | 390[e] | Cr? |
| 340 | 340 | $Cr_2$? |
| 322? | 320 | CrMo |
| 308 | Not obsd | $Mo_2$ |
| 263[f] | Not obsd | $Cr_2$ |
| 248 | Not obsd | CrMo |
| 232[f] | Not obsd | $Mo_2$ |

[a] Units in nm. [b] At 10 K, this study. [c] Gas phase, Yu. M. Efremov et al. [d] Vibronic structure is observed on this band (Figure 4) with an average spacing of 147 $cm^{-1}$. [e] Strong Cr atomic resonance absorptions appear in this region of the spectrum. [f] Careful examination of the 232/263-nm bands of $Mo_2/Cr_2$, respectively, under high concentration, high ordinate expansion conditions, reveals weak shoulders at 226/268 nm, respectively, that had not previously been noticed[10a,15] (Figure 3). Other very weak bands indicated by an asterisk in Figure 3 are not assigned because it is not possible with the available data to define them as belonging to binuclears or higher clusters.

tablished the optimum conditions for $Cr_2$ and $Mo_2$ formation in Ar matrices at 10 K and having demonstrated that under these circumstances trimer and higher clusters are expected to still be unobservable,[9,10a,15] one can assign with a fair degree of confidence the new species as the heteronuclear diatomic molecule CrMo. Convincing support for this assignment originates from the close similarity of our UV–visible data for CrMo to that obtained from the gaseous products generated from flash photolyzing $Cr(CO)_6/Mo(CO)_6$ mixtures.[18] The UV–visible data for these mixtures, which purportedly contain $Cr_2/CrMo/Mo_2$, are compared in Table I with our $Cr_2/CrMo/Mo_2$ matrix data. The correspondence for the observed bands is remarkably close.

A noteworthy feature of the observed electronic absorptions of CrMo is the close correspondence of their frequencies to those calculated under the assumption that

$$\nu_{CrMo} = {}^1/_2(\nu_{Cr_2} + \nu_{Mo_2})$$

(see Table II). Such an averaging effect of the transition energies of CrMo relative to $Cr_2$ and $Mo_2$ is intuitively understandable as the electronic ground states of Cr and Mo atoms are both $ns^1\ (n-1)d^5$ and those of $Cr_2$ and $Mo_2$ are both thought to be $1\sigma_g^2 1\pi_u^4 2\sigma_g^2 1\delta_g^4$.[15,21] Furthermore, the Cr 4s,3d and Mo 5s,4d atomic orbitals which are thought to be the main contributors to the metal–metal bonding in $Cr_2/CrMo/Mo_2$ are known to have similar energies (see Table III, Figures 5 and 7). The MO calculations described below explicitly confirm the intermediacy of CrMo energy levels between those of $Cr_2$ and $Mo_2$.

**Table II.** Predicted Energies of the Low-, Medium-, and High-Energy Transitions of CrMo under the Assumption That $\nu_{CrMo} = 1/2(\nu_{Cr_2} + \nu_{Mo_2})$

| | | (I) low | (II) medium | (III) high |
|---|---|---|---|---|
| $\nu_{obsd}$, $cm^{-1}$ | $Cr_2$ | 21 739.1 | 29 411.8 | 38 022.8 |
| | $Mo_2$ | 19 379.8 | 32 467.5 | 43 103.5 |
| | CrMo | 20 555.2 | 31 055.9 | 40 322.6 |
| $\nu_{calcd}$, $cm^{-1}$ | CrMo | 20 559.5 | 30 939.6 | 40 563.2 |

**Table III.** Parameters Used in the Extended Hückel Molecular Orbital Calculations for $Cr_2$, CrMo, and $Mo_2$

| | Orbital | Orbital exponent | $H_{ii}$, eV |
|---|---|---|---|
| Cr | 3p | 3.817 | −56.22 |
| | 3d | 3.253 | −6.80 |
| | 4s | 1.285 | −7.60 |
| | 4p | 1.200 | −3.75 |
| Mo | 4p | 3.761 | −44.39 |
| | 4d | 3.105 | −7.00 |
| | 5s | 1.409 | −7.00 |
| | 5p | 0.994 | −4.25 |

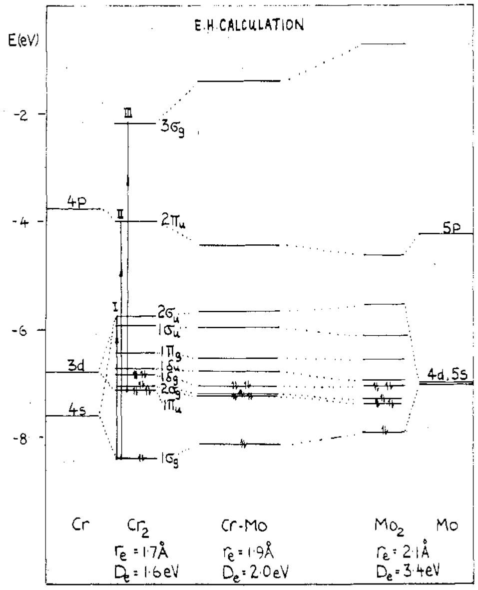

**Figure 5.** Extended Hückel molecular orbital energy level schemes calculated for $Cr_2$, $Mo_2$, and CrMo at their minimum internal energy geometries of 1.7, 2.1, and 1.9 Å, respectively.

It is pertinent to note here that the calculated $\sigma$–$\sigma^*$ transition energies for several discrete, heteronuclear *complexes* are predicted well under the assumption that

$$\sigma\text{-}\sigma^*(L_nM\text{-}M'L'_n) = {}^1/_2\{\sigma\text{-}\sigma^*(L_nM\text{-}ML_n) + \sigma\text{-}\sigma^*(L'_mM'\text{-}M'L'_m)\}$$

the point being that the position of the band for a complex such as $(\eta^5\text{-}C_5H_5)Mo(CO)_3Co(CO)_4$ is fairly accurately predicted from the assigned $\sigma$–$\sigma^*$ energies of $(\eta^5\text{-}C_5H_5)_2Mo_2(CO)_6$ and nonbridged $Co_2(CO)_8$.[22] In view of the correlation that appears to exist between $\sigma$–$\sigma^*$ energies and M–M bond strengths,[23] it has been suggested that the ability to predict M–M′ $\sigma$–$\sigma^*$ energies from those of M–M and M′–M′ complexes implies minimal ionic bonding in the heteronuclear complexes.[22] Our MO calculations indeed support the view that there is minimal charge separation in CrMo.

## Extended Hückel Molecular Orbital Calculations for $Cr_2$, CrMo, and $Mo_2$

There has been a little earlier work on transition metal diatomic molecules using the extended Hückel (EH) method.[1a,b,e,24] Two of us (W.K., G.A.O.)[15] have previously reported EH results for $Cr_2$ and $Mo_2$. In these calculations the 3p, 3d, 4s, and 4p orbitals of atomic Cr and the 4p, 4d, 5s, and 5p orbitals of atomic Mo were employed. The Coulomb integrals were parameterized to qualitatively fit the observed electronic transitions of $Cr_2$ and $Mo_2$, and the molecular orbital energies were computed as a function of internuclear distance. Using the orbital exponents[1a,26] and Coulomb integrals[1a,24b,27] listed in Table III, one calculates (using the Cusachs approximation[28]) potential energy minima at 1.7 and 2.1 Å for $Cr_2$ and $Mo_2$, respectively.[15,37,38] For these geometries, the energy level schemes shown in Figure 5 were obtained; the predicted ground state is thus $1\sigma_g^2 1\pi_u^4 2\sigma_g^2 1\delta_g^4$.

According to these energy level schemes, at least eight electronic transitions are spin and electric dipole allowed and could occur within the range of our UV–visible instrument (200–700 nm), although some are expected to be quite weak. It is thus difficult to make definitive assignments of the characteristic low- (I), medium- (II), and high-energy (III) absorptions observed for $Cr_2$ and $Mo_2$. The best one can do at this stage is to combine the spectroscopic data for the two molecules and arrive at a set of assignments that generally follows the trends of Figure 5. Such a scheme is depicted there by vertical arrows labeled I, II, and III.

We note here that the exceptionally short metal–metal distances calculated for the closed-shell configurations of $Cr_2$ (1.7 Å)[15] and $Mo_2$ (2.1 Å)[15,21] have been interpreted earlier[15,21] in terms of a formally "sextuple" bond order for the metal–metal interaction, comprising two $\sigma$, four $\pi$, and two $\delta$ components (the relative contributions of the bond overlaps remain to be established).[37] The larger calculated bond dissociation energy for $Mo_2$ (3.4 eV) compared to that of $Cr_2$ (1.6 eV) is in line with the expected trend in metal–metal bond strengths on passing from the first to the second transition series.[29] Moreover, the value for $Cr_2$ agrees remarkably well with the experimental $D_e$ value (1.56 ± 0.30 eV).[39]

As discussed earlier, UV–visible spectra indicate that the heteronuclear dimer CrMo has electronic properties intermediate between those of the parent diatomics $Cr_2$ and $Mo_2$ (Table II, Figures 2–4). This proposal receives considerable support from the results of a series of EH calculations for CrMo using the orbitals, orbital exponents, and Coulomb integrals employed to fit $Cr_2$ and $Mo_2$ (Table III, Figure 5). The resulting energy level scheme for CrMo, shown in Figure 5, immediately indicates that the electronic structure is very similar to those of $Cr_2$ and $Mo_2$. For example, if we assume the $1\sigma_g \rightarrow 2\sigma_u$, $1\sigma_g \rightarrow 2\pi_u$, and $1\pi_u \rightarrow 3\sigma_g$ assignments for bands I, II, and III, respectively, of $Cr_2$ and $Mo_2$, then analogous transitions for CrMo can be seen to occur at roughly intermediate energies. Moreover, the minimum-energy configuration for CrMo computes at 1.9 Å, which is also intermediate between the corresponding predictions for $Cr_2$ and $Mo_2$. We also find that by varying the absolute values of the atomic-orbital energies of Mo relative to those of Cr, but retaining the *n*s, *n*p, $(n-1)$d energy-level separations and internuclear distances constant, the final outcome for CrMo is not drastically affected. Finally, the bond energy estimated for CrMo, 2.0 eV, is also intermediate between the values calculated for $Cr_2$, 1.6 eV, and $Mo_2$, 3.4 eV.

## SCF–X$\alpha$ Scattered Wave Calculations for $Cr_2$, CrMo, and $Mo_2$

The difficulties of properly parameterizing extended Hückel calculations for metal clusters have been pointed out by those using them[24c] and by those who employ ab initio Hartree–Fock[30] or X$\alpha$–SW[1c,d,25] methods. We have therefore carried out SCF–X$\alpha$–SW calculations on $Cr_2$, CrMo, and $Mo_2$ in hopes of obtaining an improved description of the one-electron orbitals. Two of us (J.G.N. and H.J.K.) have previously[21] reported some of the results for $Mo_2$ along with similar studies of the quadruply bonded complex $Mo_2(O_2CH)_4$.

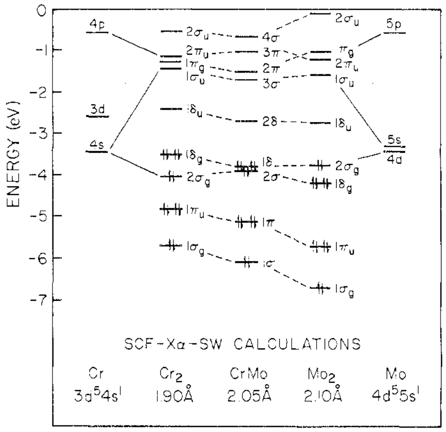

**Figure 6.** Ground-state SCF–X$\alpha$–SW energy levels for Cr, $Cr_2$, CrMo, $Mo_2$, and Mo. The molecular energy levels most closely correlating with atomic s and p levels are indicated; all others most closely correlate with d levels. Cr sphere radii were 2.380 and 2.424 bohrs in $Cr_2$ and CrMo, respectively; Mo radii were 2.576 and 2.638 bohrs in $Mo_2$ and CrMo, respectively. Touching outer-sphere radii were used.

At present we have complete ground-state calculations at bond distances of 1.90, 2.05, and 2.10 Å for $Cr_2$, CrMo, and $Mo_2$, respectively. We have also carried out explicit transition-state calculations for several spin-allowed electronic excitations of each molecule. The distance of 2.10 Å for $Mo_2$ was estimated from its apparent Mo–Mo stretching frequency[15] and is within the range of 2.09–2.18 Å established by x-ray crystallography for Mo–Mo quadruple bonds in binuclear complexes.[29] Comparison of x-ray structures for the molecules $M_2(C_3H_5)_4$, $M_2(CH_3)_8^{4-}$, and $(C_5H_5)_2M_2(CO)_6$, M = Cr, Mo,[29,31] indicates that strong Mo–Mo bonds are typically ca. 0.2 Å longer than their Cr–Cr analogues; hence we chose Cr–Cr = 1.90 Å for $Cr_2$. Our distance of 2.05 Å for CrMo seems reasonalbe in view of the fact that the metal–metal bond lengths in $CrMo(O_2CCH_3)_4$ and $Mo_2(O_2CCH_3)_4$ are 2.05 and 2.09 Å, respectively.[29,32]

Ground-state SCF energy levels for $Cr_2$, CrMo, and $Mo_2$ are compared in Figure 6 with those of Cr and Mo. All orbitals are more than 80% d in character except $2\sigma_g/2\sigma$, $1\sigma_u/3\sigma$, and $2\pi_u/3\pi$. The first of these is essentially s, the second a roughly 2:1 $d_{z^2}$:s hybrid, and the third mainly $p_{x,y}$. The $2\pi_u/3\pi$ orbital is unique in having most of its density outside the atomic regions. It is a very diffuse, "Rydberg-state" orbital. We note for later reference that electronic transitions to it are thus likely to disappear entirely in any condensed phase, including the Ar matrix in which the experimental spectra were obtained.[33]

The energies of occupied levels for CrMo are all within 0.1 eV of the averaged energy of their $Cr_2$ and $Mo_2$ counterparts, and all the occupied orbitals have nearly equal Cr and Mo character. The situation is not quite so simple for the four highest unoccupied orbitals, possibly because they can interact with each other and with lower levels in ways forbidden in the higher symmetry of the homonuclear diatomics. The splitting of the d band increases from $Cr_2$ to $Mo_2$, despite the accompanying increase in metal–metal distance; this is consistent with the expected greater intrinsic strength of the Mo–Mo bond. The *increase* in energy of the mainly s $2\sigma_g$ level from

**Table IV.** Electronic Transitions of $Cr_2$, CrMo, and $Mo_2$, as Calculated by the SCF–Xα–SW Method[a]

| Transition | Molecule | Calcd[b] | Exptl |
|---|---|---|---|
| $1\delta_g \rightarrow 1\delta_u$ | $Cr_2$ | 12.7 | |
| | $Mo_2$ | 14.4 | |
| $2\sigma_g \rightarrow 1\sigma_u$ | $Cr_2$ | 24.9 | 21.7 |
| $2\sigma \rightarrow 3\sigma$ | CrMo | 22.0 | 20.6 |
| $2\sigma_g \rightarrow 1\sigma_u$ | $Mo_2$ | 21.8 | 19.4 |
| $2\sigma_g \rightarrow 2\sigma_u$ | $Cr_2$ | 28.8 | 29.4 |
| $2\sigma \rightarrow 4\sigma$ | CrMo | 28.0 | 31.1? |
| $2\sigma_g \rightarrow 2\sigma_u$ | $Mo_2$ | 30.1 | 32.5 |
| $1\pi_u \rightarrow 1\pi_g$ | $Cr_2$ | 32.0 | *d* |
| $1\pi \rightarrow 2\pi$ | CrMo | 31.9 | *d* |
| $1\pi_u \rightarrow 1\pi_g$ | $Mo_2$ | 40.1 | *d* |
| $1\sigma_g \rightarrow 1\sigma_u$ | $Cr_2$ | 36.5 | 38.0 |
| $1\sigma \rightarrow 3\sigma$ | CrMo | 38.1 | 40.3 |
| $1\sigma_g \rightarrow 1\sigma_u$ | $Mo_2$ | 45.4 | 43.1 |
| $1\sigma_g \rightarrow 2\pi_u$ | $Cr_2$ | 40.2 | *c* |
| | $Mo_2$ | 47.1 | *c* |

[a] Band positions are in $cm^{-1} \times 10^3$. The calculated values were obtained using the relation $1\ eV = 8.06548 \times 10^3\ cm^{-1}$. [b] Explicit predictions of the singlet (spin-allowed) transitions, except for the $1\delta_g \rightarrow 1\delta_u$ and $1\pi_u \rightarrow 1\pi_g/1\pi \rightarrow 2\pi$ excitations, where the predictions are of the average transition energy to the four singlet states arising from the excited orbital configuration. [c] Could possibly be associated with the weak bands observed at 268 nm for $Cr_2$ and 226 nm for $Mo_2$, respectively. If this is in fact true, then the weak band at roughly 255 nm for CrMo (Figure 3) could be the corresponding $1\sigma \rightarrow 3\pi$ transition. [d] Either too weak to be observed or obscured by free atom absorptions (see text).

$Cr_2$ to $Mo_2$ provides an interesting contrast to the d-band behavior. This orbital, although nominally the sixth component of the sextuple bond, in practice has only very weakly bonding character. As a result, atomic rather than molecular considerations dominate its behavior; the atomic Cr 4s orbital is more stable than is its Mo 5s analogue relative to the corresponding atomic d orbitals. As discussed below, this result is helpful in assigning the electronic spectra of the diatomics.

Two of us (J.G.N. and H.J.K.) will present further details of the bonding in $Cr_2$, CrMo, and $Mo_2$, including contour maps of wave functions, potential energy curves, and a comparison with metal–metal bonded complexes, in a separate publication. Our analysis of the electronic spectra appears in Table IV. The only dipole-allowed transitions of $Cr_2$ and $Mo_2$ omitted from the table are $1\sigma_g \rightarrow 1\sigma_u$, which should occur at very high energy, and the pair $1\delta_g,2\sigma_g \rightarrow 2\pi_u$. As noted above, the diffuse Rydberg character of the $2\pi_u$ orbital makes it unlikely that transitions to it will be observed in the Ar matrix.[33] In any case, such transitions are probably quite weak due to poor overlap of localized and Rydberg orbitals. We *have* calculated the energy of the $1\sigma_g \rightarrow 2\pi_u$ transition, since it is at least conceivable that the broad, fairly weak band III is due to this excitation. However, as discussed below, the calculations more strongly support another assignment.

Discounting transitions to the $2\pi_u/3\pi$ orbital, then, we are left with four predicted excitations in the range where the three spectral bands are observed. Comparing the calculated and experimental energies, we propose that the three main bands are due to the three possible $\sigma \rightarrow \sigma^*$ transitions. The resulting agreement between theory and experiment is excellent. However, the fourth predicted transition, $\pi \rightarrow \pi^*$, cannot be ruled out as a possible assignment for either band II or III. The broad, asymmetric shape of band III (Figures 2 and 3) could be due to the fact that both the $\pi \rightarrow \pi^*$ and the third $\sigma \rightarrow \sigma^*$ excitations are contributing to it. We consider it more likely that the $\pi \rightarrow \pi^*$ transition is simply not strong enough to be observed under the experimental conditions or is obscured by free-atom absorptions.

We are particularly confident of the assignment of band I to the $2\sigma_g \rightarrow 1\sigma_u/2\sigma \rightarrow 3\sigma$ excitation, in view of the fact that both theory and experiment show a decrease in energy of this band as one moves from $Cr_2$ to $Mo_2$. As discussed above, no d → d transition should show this behavior since the d-band splitting increases from $Cr_2$ to $Mo_2$ as the intrinsic metal–metal bond strength increases. The only case for which the observed behavior is expected is for an s → d or s → ds transition, since the atomic s orbital energy increases from Cr to Mo. This is indeed the predicted character of the $2\sigma_g \rightarrow 1\sigma_u/2\sigma \rightarrow 3\sigma$ excitation.

Detailed numerical comparison of theory and experiment suggests that our assumed bond distance for CrMo is slightly too long compared to those used for $Cr_2$ and $Mo_2$. A little shorter distance would slightly increase the calculated transition energies, thus bringing those for $2\sigma \rightarrow 4\sigma$ and $1\pi \rightarrow 2\pi$ into a truly intermediate position relative to their analogues in $Cr_2$ and $Mo_2$. As noted above, we plan a study of potential curves for these molecules by the Xα–SW method to further refine our theoretical predictions. It seems very unlikely, however, that any of the spectral assignments proposed here will be altered as a result.

Our assignment of the spectra by the Xα–SW method thus differs strikingly from that arising out of the EH calculations! Comparison of Figures 5 and 6 reveals the very simple reason for this: the Xα–SW d-band splitting is about five times as great as in the EH treatment. In the latter, the levels most closely correlating with s atomic orbitals completely bracket the d band, while in the former essentially the opposite is true. This result is actually not surprising in view of similar previous observations by those studying larger metal clusters. Direct comparison of EH and Xα–SW energy levels for $Ni_{13}$, e.g., shows that the conventional EH parameterization leads to a d-band splitting which is much too small.[1c,d] Moreover, comparison of Xα–SW ionization energies for $Mo_2(O_2CH)_4$ with photoelectron spectra shows that the d-band splitting predicted by the calculation is essentially identical with that observed experimentally.[21] We thus feel that the Xα–SW calculations provide a more realistic guide to the one-electron energy levels of $Cr_2$, CrMo, and $Mo_2$ than does the EH treatment.

## Relevance of Small, Well-Defined, Heteronuclear Cluster Research to Alloy and Bimetallic Catalysis

Metal alloys continue to spur theoreticians and experimentalists into studying electronic "ligand factors" and geometric "ensemble factors" in catalysis.[1-6,34] The former is considered to affect the strength of adsorbate–adsorbent interactions while the latter influences the relative numbers of various types of atom, diatom, etc. sites available at the surface of the catalyst. Both can contribute to marked activity and selectivity changes as alloy composition is altered. Other factors, however, have to be taken into consideration in multicomponent metal systems which relate to the mode of preparation of the alloy catalyst and the miscibility of the metal components as a function of composition and cluster size. The former concerns whether the alloy is produced in the form of films, wires, ribbons, powders, or supported/unsupported aggregates (usually 10–1000 Å range). The latter involves problems of phase separation and whether before or during the course of a catalytic reaction the bulk composition of the "alloy" is truly representative of the surface composition.[2,41]

With mixed-metal systems that form a continuous series of solid solutions over the entire composition range (i.e., completely miscible), phase separation is not usually a problem. To avoid complications with partially miscible metals one tries to work within the miscibility gap. However, with totally immiscible metals, phase separation in the bulk form cannot be escaped. In this context and of considerable practical and fundamental interest is Sinfelt's work[34,35] with high-dispersion, multicomponent metal catalysts whose constituent metals are totally immiscible in the bulk. Supported and unsupported mixed-metal catalysts of this type often have remarkably different chemical properties to those of the individual metals by themselves and have led to the concept of "bimetallic" cluster catalysis. Whether the metals are miscible in "small particle form" or whether one component simply forms a coating on the surface of the second one are questions that have yet to be fully resolved.

Let us briefly recall Sinfelt's data for Cu/Ru catalysts. These are completely immiscible in the bulk, yet there is catalytic evidence of a definite interaction between the two in both supported and unsupported, high-dispersion catalysts.[35] Catalytic and chemisorption tests of this type have usually been employed to examine this question of alloying.[34e] However, proof of the reality of bimetallic clusters in supported catalysts ideally requires that the electronic environment of at least one of the atomic components be established. It seems likely that Mössbauer[36] and possibly EXAFS techniques[40] will contribute significantly to these aspects of alloy catalysis in the near future.

In the context of the present study, it is our contention that a rather unique way of looking at such "alloy" problems is through the eye of mixed-metal atom–matrix aggregation experiments coupled with an appropriate form of spectroscopy and molecular orbital theory.

In principle here one is able to answer the question as to whether the atoms of a two-component metal system can actually form "normal chemical bonds" with one another but in the few-atom regime. One can then inquire as to how these heteronuclear "molecules" compare electronically with their single-component analogues. Undoubtedly, the CrMo molecule of the present study can be considered to be a normal molecule with electronic, bonding, and chemical properties intermediate between those of $Cr_2$ and $Mo_2$. This is understandable for two electronically compatible metals like Cr and Mo which are completely miscible in the bulk. On these grounds one might anticipate that the properties of larger $Cr_xMo_y$ ($x = 1, 2, 3, ...; y = 1, 2, 3, ...$) clusters would be reasonably predicted from CrMo as a reference point (we hope to explore this idea by searching for $Cr_2Mo$ and $CrMo_2$ in higher concentration mixed-metal experiments).[10b]

Therefore in Sinfelt's terminology mixed Cr/Mo particles (supported or unsupported in the 10–1000 Å range) would be regarded as "bimetallic" clusters and CrMo can certainly be considered to be the "embryonic" cluster of the Cr/Mo alloy system. It will be fascinating to explore these ideas further by working with mixed-metal systems with disparate electronic and miscibility properties. By searching for heteronuclear metal diatomics of this type one might be able to discover whether or not two metals, which are totally immiscible in the bulk phase, can form recognizable chemical bonds in discrete MM′ molecules.

## Conclusion

Just as studies on metal-alloy catalysts constituted an important chapter in the historical development of heterogeneous catalysis, we believe that experimental and theoretical studies of heteronuclear metal clusters at the "few-atom extreme" can provide a valuable reference point on which to base one's future understanding of the complex phenomenon of "alloying" on the chemisorptive and catalytic capacity of multicomponent metal catalysts as a function of composition and structure.

**Acknowledgment.** We gratefully acknowledge the financial assistance of the National Research Council of Canada and the Atkinson Foundation (W.K. and G.A.O.) and the U.S. National Science Foundation (J.G.N. and H.J.K.). This research was completed while G.A.O. was a Sherman-Fairchild Distinguished Scholar at California Institute of Technology. The hospitality of the Chemistry Division of California Institute of Technology is greatly appreciated.

**Registry No.** CrMo, 61642-16-8; $Cr_2$, 12184-82-6; $Mo_2$, 12596-54-2; Cr, 7440-47-3; Mo, 7439-98-7.

## References and Notes

(1) (a) R. C. Baetzold, *J. Chem. Phys.*, **55**, 4363 (1971); *J. Catal.*, **29**, 129 (1973); *Surf. Sci.*, **51**, 1 (1975); (b) R. C. Baetzold and R. E. Mack, *J. Chem. Phys.*, **62**, 1513 (1975); (c) R. P. Messmer, S. K. Knudson, K. H. Johnson, J. B. Diamond, and C. Y. Yang, *Phys. Rev. B*, **13**, 1396 (1976); (d) R. P. Messmer, C. W. Tucker, Jr., and K. H. Johnson, *Chem. Phys. Lett.*, **36**, 423 (1975); (e) G. Blyholder, *Surf. Sci.*, **42**, 249 (1974), and references therein.

(2) T. E. Madey, J. T. Yates, Jr., D. R. Sandstrom, and R. J. H. Voorhoevre in "Solid State Chemistry", Vol. 2, B. Hannay, Ed., 1976, p 1, and references therein.

(3) G. C. Bond, "Catalysis by Metals", Academic Press, London and New York, 1962, and references therein.

(4) (a) A. A. Balandin, *Adv. Catal.*, **19**, 1 (1969); (b) M. Boudart, *ibid.*, **20**, 153 (1969); (c) G. A. Somorjai, *Catal. Rev.*, **1**, 87 (1972), and references therein.

(5) (a) L. H. Little, "Infrared Spectra of Adsorbed Species", Academic Press, London, 1966; (b) M. L. Hair, "Infrared Spectroscopy in Surface Chemistry", Marcel Dekker, New York, N.Y., 1967; (c) R. Ugo, *Catal. Rev.*, **11**, 225 (1975); (d) E. L. Muetterties, *Bull. Soc. Chem. Belg.*, **84**, 959 (1975); (e) G. A. Ozin, *Acc. Chem. Res.* **10**, 21 (1977); (f) "Catalysis Progress in Research", F. Basolo and R. L. Burwell, Jr., Ed., Plenum Press, New York, N.Y., 1973; (g) J. E. Demuth and D. E. Eastman, *Phys. Rev. Lett.*, **32**, 1123 (1974); (h) H. Conrad, G. Ertl, H. Knözinger, J. Küppers, and E. E. Latta, *Chem. Phys. Lett.*, **42**, 115 (1976), and references therein.

(6) J. H. Sinfelt, *J. Catal.*, **29**, 308 (1973); *Prog. Solid State Chem.*, **10**, 55 (1975).

(7) M. Moskovits and G. A. Ozin, Ed., "Cryochemistry", Wiley, New York, N.Y., 1976.

(8) R. Busby, W. Klotzbücher, and G. A. Ozin, *J. Am. Chem. Soc.*, **98**, 4013 (1976).

(9) A. Ford, H. Huber, W. Klotzbücher, E. P. Kündig, M. Moskovits, and G. A. Ozin, *J. Chem. Phys.*, **66**, 524 (1977).

(10) (a) E. P. Kündig, M. Moskovits, and G. A. Ozin, *Nature (London)*, **254**, 503 (1975); (b) W. Klotzbücher and G. A. Ozin, *J. Mol. Catal.*, in press.

(11) (a) T. C. DeVore, A. Ewing, H. F. Franzen, and V. Calder, *Chem. Phys. Lett.*, **35**, 78 (1975); (b) S. Mitchell and G. A. Ozin, in preparation.

(12) C. McLaren, W. Klotzbücher, L. A. Hanlan, and G. A. Ozin, unpublished work.

(13) (a) H. Huber, G. A. Ozin, and W. J. Power, *J. Am. Chem. Soc.*, **98**, 6508 (1976); (b) J. Hulse and M. Moskovits, *J. Chem. Phys.*, **66**, 3988 (1977).

(14) (a) H. Huber, E. P. Kündig, M. Moskovits, and G. A. Ozin, *J. Am. Chem. Soc.*, **97**, 2097 (1975); (b) G. A. Ozin, *Appl. Spectrosc.*, **30**, 573 (1976); (c) H. Huber and G. A. Ozin, *Inorg. Chem.*, in press.

(15) W. Klotzbücher and G. A. Ozin, *Inorg. Chem.*, **16**, 984 (1977).

(16) L. A. Hanlan and G. A. Ozin, *Inorg. Chem.*, in press.

(17) W. Klotzbücher, W. J. Power and G. A. Ozin, manuscript in preparation.

(18) Yu. M. Efremov, A. N. Samoilova, and L. V. Gurvich, *Chem. Phys. Lett.*, **44**, 108 (1976).

(19) E. P. Kündig, M. Moskovits, and G. A. Ozin, *J. Mol. Struct.*, **14**, 137 (1972); M. Moskovits and G. A. Ozin, *J. Appl. Spectrosc.*, **26**, 481 (1972).

(20) W. Klotzbücher, H. Huber, and G. A. Ozin, *Rev. Sci. Instrum.*, in press.

(21) J. G. Norman, Jr., H. J. Kolari, H. B. Gray, and W. C. Trogler, *Inorg. Chem.*, **16**, 987 (1977).

(22) H. B. Abrahamson, C. C. Frazier, D. S. Ginley, H. B. Gray, J. Lilienthal, D. R. Tyler, and M. S. Wrighton, *Inorg. Chem.*, **16**, 1554 (1977).

(23) (a) D. DeWit, J. P. Fawcett, A. J. Poe, and M. V. Twigg, *Coord. Chem. Rev.*, **8**, 81 (1972); (b) J. P. Fawcett, A. J. Poe, and M. V. Twigg, *J. Chem. Soc., Chem. Commun.*, 267 (1973).

(24) (a) R. Hoffmann, *J. Chem. Phys.*, **39**, 1397 (1963); (b) W. F. Cooper, G. A. Clarke, and C. R. Hare, *J. Phys. Chem.*, **76**, 2268 (1972); C. R. Hare, T. P. Sleight, W. F. Cooper, and G. A. Clarke, *Inorg. Chem.*, **7**, 669 (1968), and references therein; (c) A. B. Anderson, *J. Chem. Phys.*, **64**, 4046 (1976); **65**, 1729 (1976), and references therein.

(25) N. Rösch and T. N. Rhodin, *Faraday Discuss. Chem. Soc.*, **58**, 28 (1974).

(26) E. Clementi and D. L. Raimondi, *J. Chem. Phys.*, **38**, 2686 (1963); E. Clementi and J. Roetti, *At. Nucl. Data Tables*, **14**, 445 (1974).

(27) I. Baranovskii and A. B. Nikol'skii, *Teor. Eksp. Khim.*, **3**, 527 (1967).

(28) L. C. Cusachs, *J. Chem. Phys.*, **43**, S157 (1965).

(29) F. A. Cotton, *Chem. Soc. Rev.*, **4**, 27 (1975); *Acc. Chem. Res.*, **2**, 240 (1969).

(30) (a) P. Joyes and M. Leleyter, *J. Phys. B*, **6**, 150 (1973); (b) C. F. Melius, J. W. Moskovitz, A. P. Mortola, M. B. Baillie, and M. A. Ratner, *Surf. Sci.*, **59**, 279 (1976).

(31) R. J. Klinger, W. Butler, and M. D. Curtis, *J. Am. Chem. Soc.*, **97**, 3535 (1975).

(32) C. D. Garner, R. G. Senior, and T. J. King, *J. Am. Chem. Soc.*, **98**, 3526 (1976).

(33) J. M. Schurr, *Int. J. Quantum Chem.*, **2**, 221 (1971).

(34) (a) V. Ponec and W. M. H. Sachtler, *J. Catal.*, **24**, 250 (1972); (b) J. S. Campbell and P. H. Emmett, *ibid.*, **7**, 252 (1967); (c) J. H. Sinfelt,

J. L. Carter, and D. J. C. Yates, *ibid.*, **24**, 283 (1972); (d) J. K. Clarke, *Chem. Rev.*, **75**, 291 (1975); (e) M. Prunet, M. V. Mathieu, and W. M. H. Sachtler, *J. Catal.*, **44**, 324 (1976), and references therein.

(35) J. H. Sinfelt, Y. L. Lam, J. A. Cusumano, and A. E. Barnett, *J. Catal.*, **42**, 227 (1976), and references therein.

(36) R. L. Garten, *J. Catal.*, **43**, 18 (1976), and references therein.

(37) It is reassuring to note here that a rotational analysis of the 4600 Å region of $Cr_2$ [Yu. M. Efremov, A. N. Samoilova, and L. V. Gurvich, *Opt. Spectrosc.* (*USSR*), **36**, 381 (1974)] generated by flash photolysis of gaseous $Cr(CO)_6$, yields an internuclear separation of 1.71 Å, which is reasonably close to the minimum energy distance calculated in our EH (1.7 Å) and used in our Xα–SW (1.9 Å) calculations. Moreover, the resolved rotational structure of the 4600 Å band of $Cr_2$ resembles that of a single, headless band characteristic of a $^1\Sigma_g \rightarrow {}^1\Sigma_u$ electronic transition as predicted by the calculations.

(38) Note that the VOIP's employed for the $Cr_2$ calculations of the present study are slightly different than those used in ref 15.

(39) A. Kant and B. Strauss, *J. Chem. Phys.*, **45**, 3161 (1966).

(40) S. P. Cramer, T. K. Eccles, F. Kutzler, K. Hodgson, and S. Doniach, *J. Am. Chem. Soc.*, **98**, 8059 (1976).

(41) See, for example, W. M. H. Sachtler and R. A. van Santen, *Adv. Catal.*, **26**, 69 (1977).

---

Contribution from the Department of Chemistry,
Kent State University, Kent, Ohio 44242

# Electron Transfer through Organic Structures. 29. A Reversed Acidity Pattern in Carboxylato-Bridged Reductions by Vanadium(II)[1]

MARILYN K. LOAR, JEAN C. THOMAS, JOHN W. REED, and EDWIN S. GOULD*

*Received April 17, 1977*

AIC702821

The reductions of several (di- and (trialkylacetato)pentaamminecobalt(III) complexes with $V^{2+}$ (25 °C, $\mu = 4.0$) are accelerated as $[H^+]$ is increased from 0.10 to 4.0 M, a reversal of the acidity pattern ordinarily observed for reactions of this type. After correction of the trialkyl, but not the dialkyl, derivatives for kinetic medium effects, the reductions conform to a rate law (eq 1) pointing to partition of the cobalt into a nonprotonated and a more rapidly reacting protonated form. The observed reversal arises because the increased branching at the α carbon of the carboxyl ligand has depressed the specific rate of the nonprotonated bridged component below that of the protonated outer-sphere path (which is much less sensitive to nonbonded interactions). Acidity constants for the protonated forms of the oxidants have been evaluated, as have specific rates for the two forms of each oxidant. The acidities of the branched oxidants are found to lie above those for the straight-chain acetato and propionato complexes, probably reflecting the greater difficulty in solvating the protonated (tripositive) forms bearing bulky lipophilic groups.

Although the mediating action by carboxyl ligands on the inner-sphere reductions of bound cobalt(III) can be significantly altered by protonation,[2] the resulting dependencies are at present inadequately understood. In particular, when the basic site is conjugated with $COOCo^{III}$ but lies out of the path of electron transfer, protonation may increase[3] or decrease[4] the rate of reduction, but the electronic features which govern the direction of the effect have not been defined. In cases where electron transfer occurs through an extended segment of the ligand (remote attack), protonation often accelerates the reaction,[5] but, again, no convincing rationale for this rate enhancement has yet appeared. The picture is more straightforward for reactions proceeding through chelated transition states, for here protonation simply ties off a basic site in the oxidant where chelation might otherwise occur.[6] Finally, when the lead-in function constitutes the only basic site in the bridging ligand, attachment of $H^+$ blocks off the bridged path, leaving only an outer-sphere route for the protonated oxidant.

The latter description applies to the reductions, using $Cr^{2+}$, $Eu^{2+}$, and $V^{2+}$, of the acetato and propionato derivatives of $(NH_3)_5Co^{III}$, each of which is strongly retarded at high acidities. Earlier studies[7,8] yielded values for the acidity constants of these oxidants and indicated that the ratio of specific rates, $k_V/k_{Eu}$, associated with reductions of the protonated forms, corresponds closely to the ratios observed for known outer-sphere series.[9] It was further suggested that since the inner-sphere path is much more sensitive than the outer-sphere to the degree of alkylation in the carboxyl group,[9] it should be possible, by increasing branching, to depress the specific rate of the bridged component below that of the protonated outer-sphere path. In such instances, protonation would accelerate, rather than retard, reaction, and a reversal of the usual acidity pattern for this type of system would result. We here report several examples of such an inversion.

## Experimental Section

**Materials.** Solutions of V(II) were prepared and analyzed as described.[10] Cobalt complexes not available from previous studies[9,11] were prepared by known methods.[9,12] Lithium perchlorate was prepared as described.[13] Ligands (Aldrich, K&K, or Pfaltz and Bauer products) were used without purification.

**Rate Measurements.** Rates were estimated from measurements of absorbance decreases on the Cary 14 spectrophotometer as described.[7,10a,11] Measurements were made at 502 nm. Reactions were first order each in Co(III) and $V^{2+}$, but rate measurements were carried out under pseudo-first-order conditions with at least a tenfold excess of $V^{2+}$. Ionic strengths were adjusted using twice-recrystallized $LiClO_4$. To minimize volume changes resulting from mixing reagents, the solution containing $V(ClO_4)_2$, perchloric acid, and lithium perchlorate was made up to the appropriate volume, and a known volume of a concentrated solution of the Co(III) complex was added using a small calibrated syringe. Reactions were followed for at least 5 half-lives. Rate constants evaluated from successive half-life values within a single run generally agreed to within 3%. Except as noted below, no trends indicative of systematic errors were observed, and average values did not differ significantly from those obtained from least-squares treatment of logarithmic plots of absorbance differences against reaction time. Specific rates obtained from replicate runs checked to within 5%. Temperatures were kept at 25.0 ± 0.2 °C during the entire series of experiments.

The V(II) reductions of the chloroacetato, trichloroacetato, and heptafluorobutyrato complexes of $(NH_3)_5Co^{III}$ did not give simple kinetic curves. Stoichiometry studies[12] indicated that reductions of the chlorinated complexes were complicated by competing reduction of bound chlorine in a manner analogous to that described for $Cr^{2+}$ reductions.[7] The source of difficulty with the fluorinated derivative is less clear, but we suspect that this complex undergoes significant aquation, as well as reduction, in the reaction media employed.

## Results and Discussion

Kinetic data for reductions at various acidities appear in Tables I–III. The rates listed in Table I are independent of acidity or exhibit a dependence which is too slight to be ki-